Different behavior of Platinum nanoparticles (Pt NPs) catalyzed alcohol (Methanol, Ethanol, 2-Propanol and 2-Butanol) oxidation at Pt-gas and Pt-liquid interfaces: Pt NPs size, water coadsorption and alcohol concentration do matter

Hironori Tatsumi, [‡,‖] *Fudong Liu,* [‡,§,‖] *Hui-Ling Han,* [‡] *Lindsay M. Carl,* [†,‡] *Andras Sapi,* [‡,⊥] *and Gabor A. Somorjai*,* [†,‡]

[†]Department of Chemistry, University of California, Berkeley, California 94720 and [‡]Lawrence Berkeley National Laboratory, Berkeley, California 94720, United States

ABSTRACT: Platinum nanoparticles size range from 1 to 8 nm deposited on mesoporous silica MCF-17 catalyzed alcohol oxidations were studied in the gas and liquid phases. Among methanol, ethanol, 2- propanol and 2-butanol reactions, the turnover frequency increased with Pt nanoparticle size for all the alcohols utilized. The activation energies for the oxidations were

almost same among all alcohol species, but higher in the gas phase than those in the liquid phase. Water coadsorption poisoned the reaction in the gas phase, while it increased the reaction turnover rates in the liquid phase. Sum frequency generation (SFG) vibrational spectroscopy studies and DFT calculations revealed that the alcohol molecules pack horizontally on the metal surface in low concentrations and stand up in high concentrations, which affects the dissociation of β-hydrogen of the alcohols as the critical step in alcohol oxidations.

1.   INTRODUCTION

The catalytic alcohol oxidation process is crucial step for carbonyl compound production and energy conversion in the   past decades, research has been focusing on developing catalyst performance, decreasing process cost, creation of new material, and further employing alcohols as new energy sources for fuel cells.[1–3] Although there are variable ways to carry out the oxidation reactions, using transition metal catalyst with molecular oxygen is one of the promising systems to achieve productivity and low environmental impact. [4–8]

Alcohol oxidation reaction processes with heterogeneous catalysts occur in the gas-solid and liquid-solid interfaces. The reaction rate and product selectivity are significantly affected by the phase[9] and we have studied alcohol oxidation by using size controlled platinum nanoparticles (Pt NPs) and sum-frequency generation (SFG) vibrational spectroscopy techniques.[10–14] Here we report our investigation of methanol, ethanol, 2-propanol and 2-butanol oxidation reactions and summarize these results, which gives us the general knowledge on how each alcohol molecule behaves on the catalyst surface in various conditions.

2. EXPERIMENTAL SECTION

2.1. Size Control of Platinum nanoparticles (Pt NPs) loaded in MCF-17

Pt NPs were synthesized by PVP-assisted polyol process in ethylene glycol.[10–12,14] The average sizes for the nanoparticles are 1, 2, 4, 6 and 8 nm respectively with narrow size distributions as determined by transmission electron microscopic (TEM) images. In order to study the catalytic alcohol oxidation reaction with molecular oxygen in the gas and liquid phases, we chose the mesoporous silica MCF-17 as the Pt support.[15,16] MCF-17 has wide pore size ranges from 15 to 50 nm which are adequate to incorporate the sub 10 nm Pt NPs. The amount of Pt loaded into the supports was measured by inductively coupled plasma atomic emission spectroscopy (ICP-AES). The mass loadings of Pt in each catalyst were from 0.4 to 0.7 wt. %.

2.2. Thin film Pt catalyst for Sum frequency generation analysis

The samples for 2-propanol oxidation were prepared by depositing Langmuir-Blodgett films[17,18] of silica embedded 4 nm Pt nanoparticles on sapphire prisms followed by calcination in air at 550 °C for 3h. To prepare 4 nm Pt nanoparticles embedded in silica, Pt nanoparticle ethanol suspension and tetraethyl orthosilicate were mixed with ethanol, to which ammonium hydroxide was added drop-wise within 5 min under stirring. The mixture was then sonicated for 2 h. The product was precipitated by hexane and collected by centrifugation. [12]

2.3. Catalytic Oxidation Studies

Various alcohol oxidation reactions were investigated in the gas and liquid phases using Pt NPs loaded into MCF-17 with pure anhydrous alcohol; methanol, ethanol, 2-propanol and 2-butanol from Aldrich. For gas phase catalysis, the reactions were carried out in a gold-coated

batch-reactor equipped with a boron nitride substrate heater and a metal bellows circulation pump for gas mixing. Each catalyst was dispersed in ethanol and drop-casted on SiO_2 chips, and then set on a boron nitride substrate heater. The reactor was typically filled with 10 Torr of alcohol, 50 Torr of oxygen and 710 Torr of helium at 60 °C. The products were detected by a gas chromatography (GC) with a thermal conductivity detector.

For liquid phase catalysis, the reactions were carried out in a 100 ml stirred Parr reactor covered by heating tape. The reactor was typically filled with 10–30 mg of Pt/MCF-17 catalyst dispersed in 15 ml of liquid alcohol. The mixture was sealed, purged by pure oxygen, and then sealed at 1 bar oxygen atmosphere. Magnetic stirring was set at a certain speed and the mixture was kept at 60 °C. For 2-butanol oxidation reaction, typical oxygen pressure was 3 bar, and the reaction temperature was 80°C. After 1–3 h of reaction, the reactor was cooled to 45 °C. The gas in the reactor was transferred into the evacuated gas-phase reactor connected to the GC to analyze the reactants and products in the gas phase. The liquid in the reactor was centrifuged to remove the solid catalyst. The supernatant was then injected into the GC to analyze the reactants and products in the liquid phase.

For the gas-phase reaction, the product selectivity and turnover frequency (TOF) were typically calculated at alcohol conversions under 30 %. For the liquid-phase reaction, the product selectivity and TOF were typically calculated at oxygen conversions between 20–40 % (corresponding alcohol conversions between 1–4 %). Number of active sites for each catalyst was calculated based on the TEM (particle size) and ICP-AES (Pt loading) data, assuming spherical nanoparticles and the same atomic density on the Pt nanoparticle surface as Pt (111).

The products of the methanol oxidation reaction were carbon dioxide (CO_2), formaldehyde and methyl formate as a coupling product. The products of the other alcohol oxidation reactions were CO_2 and corresponded carbonyl compounds; acetaldehyde (Ethanol), acetone (2-Propanol) and 2-butanone (2-Butanol). No acid and ester products were detected in our experiments.

2.4. Sum frequency generation vibrational spectroscopy

Sum frequency generation (SFG) vibrational spectroscopy is using secondary nonlinear optical effect, which is highly selective toward the interfaces. This is one of the effective techniques to obtain the molecular orientations on the catalyst surface under reaction conditions. In our experiments, the infrared frequency was scanned from 2800 to 3600 cm^{-1} and its energy was ~100 µJ. The nonresonant frequency used was 532 nm (40 µJ). Sum frequency light was detected by a photomultiplier connected with a gated integrator. The polarization combination used in the experiment was ppp, which refers to perpendicular polarization for all beams relative to the sample surface. The data points in the spectra shown in this paper typically are comprised of an average of 400−1000 individual measurements. In the 2-propanol SFG analysis, the reaction phase effect was examined under reaction condition. For the gas phase analysis, the sample was placed in the cell, then pure oxygen was bubbled through 2-propanol and sent through the cell at 18°C. For the liquid phase analysis, liquid 2-propanol was passed through the cell using a peristatic pump.

3.   RESULTS AND DISCUSSION

3.1. Reaction Rate Comparison of Catalytic Alcohol Oxidation Reactions in the Gas and Liquid Phases

Each turnover frequency (TOF) values of alcohol oxidation reactions were summarized in order to reveal the correlation among the carbon number, reaction phase and reaction turnover rate. Figure 1 shows the TOF over 6 nm Pt NPs loaded in MCF-17 in the gas and liquid phases. The total TOF sums up the number of the whole reaction product's TOF. In the gas phase reaction, methanol oxidation result shows the highest TOF value; 10 molecules·site^{-1}·s^{-1} among C1-C4 alcohol oxidation reactions, whereas the other TOFs were 3.2 (Ethanol), 1.2 (2-Propanol) and 1.3 molecules·site^{-1}·s^{-1} (2-Butanol) respectively. In the liquid phase, the TOF values of alcohol oxidation reaction were 0.9 (Methanol), 2.1 (Ethanol), 0.2 (2-Propanol) and 1.5 molecules·site^{-1}· s^{-1} (2-Butanol: 3 bar O_2, 80°C) respectively.

The molecular amount ratios of alcohol to oxygen were 1 to 5 in the gas phase (0.8 mmol of alcohol vs 4.1 mmol of O_2), however those ratios in the liquid phase were higher than those in the gas phase due to the much higher alcohol density (Methanol Ox.: 591 mmol of methanol vs 0.2 mmol O_2, Ethanol Ox.: 413 mmol of ethanol vs 0.2 mmol O_2, 2-Propanol Ox.: 320 mmol of 2-propanol vs 0.2 mmol O_2, 2-Butanol Ox.: 250 mmol of 2-butanol vs 0.6 mmol of O_2). In order to mitigate the contrast, the alcohol was diluted with heptane to 1:1000 ratios in the liquid phase; Alcohol vs O_2 ratios were 1:0.9 (Methanol), 1:1.3 (Ethanol) and 1:1.7 (2-Propanol). Heptane is used as a neutral solvent which has small effect on reaction rate, size dependence, and activation energy in these reactions.[11,12] The TOFs in the liquid phase after heptane dilution were 0.001 (Methanol), 0.04 (Ethanol) and 0.004 molecules·site^{-1}·s^{-1} (2-Propanol) respectively, which exhibits 80~10000 times lower activity compared to the gas phase reaction under comparable concentration conditions. Although the reactant contents ratios are not same between in the gas phase and in the liquid phase (diluted), these results suggests that the alcohol molecular density has great impact on the alcohol oxidation reaction kinetics.
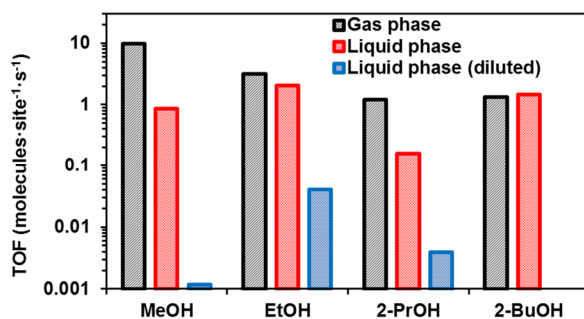
Figure 1. The total TOFs of alcohol oxidation reactions over 6 nm Pt/MCF-17. Gas phase: 10 Torr alcohol, 50 Torr O_2, He as balance, in total 770 Torr, 60 °C, Liquid phase: 15 ml pure alcohol, C1-C3 alcohol: dissolved oxygen under 1 bar, 60 °C, 2-BuOH: dissolved oxygen under 3 bar, 80 °C, Liquid phase (diluted): 15ml heptane, 15µl alcohol and dissolved oxygen under 1 bar, 60 °C

3.2. Activation Energy Comparison of Catalytic Alcohol Oxidation Reactions in the Gas and Liquid Phases

The activation energies of alcohol oxidation reactions over 4nm Pt/MCF-17 catalyst were summarized in Figure 2. In the gas phase, the activation energies were found to be 190 (Methanol), 200 (Ethanol), 147 (2-Propanol) and 120 kJ/mol (2-Butanol) respectively. Interestingly, these values became 2~6 times lower in the liquid phase; 30 (Methanol), 39 (Ethanol), 62 (2-Propanol) and 64 kJ/mol (2-Butanol) respectively. These different activation energies correlated with the reaction phase suggest different reaction mechanisms in the gas−solid and liquid−solid interface, which is discussed in detail as below; SFG Analysis and DFT calculation sections. However there are still unreasonable phenomena in the correlation between TOF value and activation energy; the big TOF gives the big activation energy, it seems to be due to the low collision frequency of oxygen on the catalyst surface. In the gas phase, any

7

reactant molecule can reach to the catalyst surface. However the catalyst is covered by large amount of solvent; alcohol and/or heptane in the liquid phase, the oxygen has difficulty in attaching to the reaction active site. Besides the gas pressure, temperature/heat transfer, and also the another pre-exponential factor may affect the apparent reaction rates.
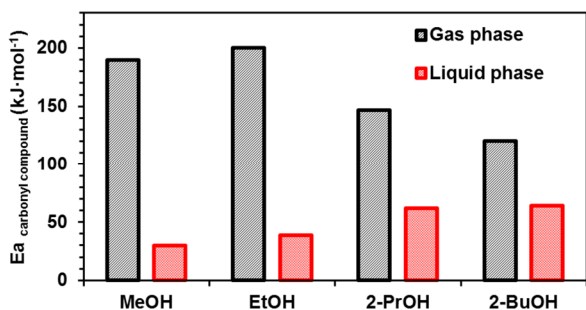

Figure 2. Activation energies of carbonyl compounds; formaldehyde (Methanol), acetaldehyde (Ethanol), acetone (2-Propanol) and 2-butanone (2-Butanol) in the gas and liquid phase alcohol oxidation reactions over 4 nm Pt/MCF-17

3.3. Influence of Pt Nanoparticle Size on Reaction Rate and Product Selectivity

In this section, we summarized the Pt NPs size dependence on the TOF and product selectivity of catalytic alcohol oxidation reactions. The relative TOF value, which helps visually to identify the trends, bases on the smallest NPs sized TOF value in each different sized alcohol oxidation reactions.
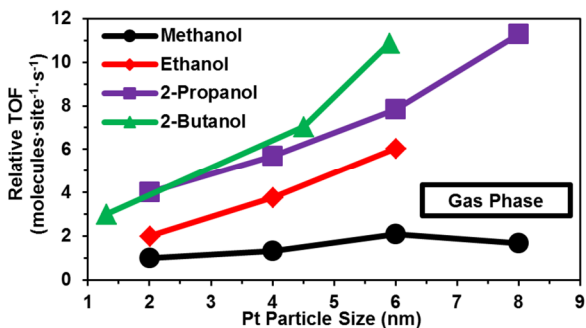
Figure 3. Size dependence of total TOFs in the gas phase (10 Torr alcohol, 50 Torr O_2, He as balance, in total 770 Torr, 60 °C)
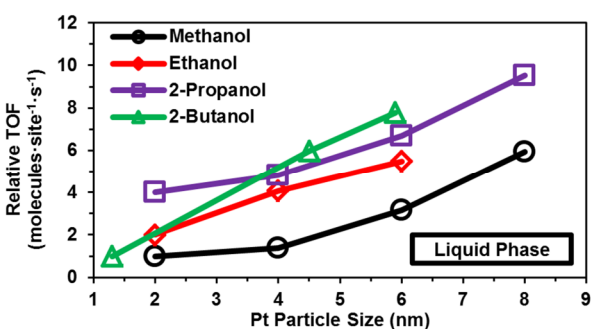

Figure 4. Size dependence of total TOFs in the liquid phase (15 ml pure alcohol, C1-C3 alcohol: dissolved oxygen under 1 bar, 60 °C, 2-BuOH: dissolved oxygen under 3 bar, 80 °C)

In the gas phase, the relative TOFs became 3~4 times larger as the particle size increases in C2-C4 alcohol cases, while it remained as similar in the methanol oxidation reaction. In the liquid phase, the relative TOFs of all alcohol oxidation reactions became big brought as the size of the Pt NPs increase (Figure 3 and Figure 4).

The selectivity toward carbonyl compound products were summarized in Figure 5. In the gas phase, it showed 21-37% for formaldehyde (Methanol), 97% for acetaldehyde (Ethanol), 100% for acetone (2-propanol) and 100% for 2-butanone (2-butanol) in the 1-8 nm range alcohol

oxidation reactions. As a result, the Pt particle size didn't affect the reaction selectivity. Most of the alcohols were converted towards corresponding carbonyl compounds. The significantly lower selectivity of methanol oxidation is due to the high activity of formaldehyde which can convert to methyl formate and CO_2.[10,19,20]
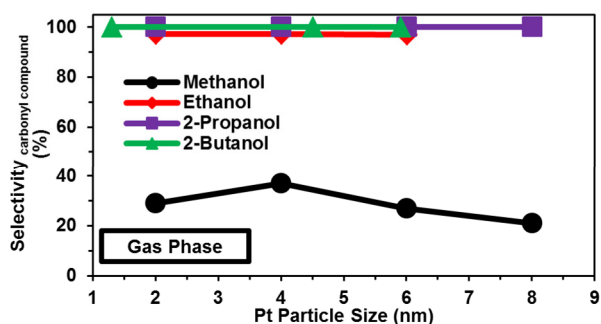

Figure 5. Size dependence of product selectivity in the gas phase (10 Torr alcohol, 50 Torr O_2, He as balance, totally 770 Torr, 60 °C) Carbonyl compound: formaldehyde (Methanol), acetaldehyde (Ethanol), acetone (2-Propanol) and 2-butanone (2-Butanol)

3.4. Water Coadsorption Effect on Reaction Rate and Product Selectivity

Water is one of the by-products of alcohol oxidation reactions; it may influence the reaction turnover rates and its coadsorption effect on the reaction progress. Therefore we studied the water addition effect on the alcohol oxidation reaction in the gas and liquid phases, which revealed unique characteristics. For the gas phase, 1−10 Torr water vapor was introduced with 10 Torr of alcohol and 50 Torr of oxygen over 4 nm Pt NPs loaded in MCF-17, dramatic loss of catalytic activity was observed in C1-C3 alcohol oxidation reactions. Especially 1 Torr of added water vapor ($X_{water\ ratio}$= 0.1) resulted in as low as 36 (Methanol) and 27% (2-Propanol) of the water-free reaction activity (Figure 6A). In C1-C3 alcohol oxidation reaction, the relative TOFs decreased to 0 when the water ratio is equal to each alcohol quantity, which means catalyst

active sites were fully covered by the water. No alcohol could reach the Pt surface. When using 6 nm Pt NPs loaded in MCF-17, different tendency was shown in the 2-butanol oxidation reaction in the gas phase. The water didn't poison the reaction, the relative TOF still remained 84% of the water-free reaction activity at $X_{water\ ratio}= 1$. In the liquid phase alcohol oxidation reaction, water coadsorption effect on the TOF showed different tendency in each case (Figure 6B). In the methanol and ethanol oxidation reactions, the relative TOFs were gradually decreased to 0 when the water ratio was equal to each alcohol quantity. In the 2-propanol oxidation reaction, the relative TOFs were increased 4 times higher compared to pure liquid alcohol by added water ($X_{water\ ratio}= 0.8$). Further increment in the water concentration resulted in the decline of activity. In the 2-butanol oxidation reaction, only 1 ml water affected the relative TOF decrease to 12% of the water-free reaction activity.
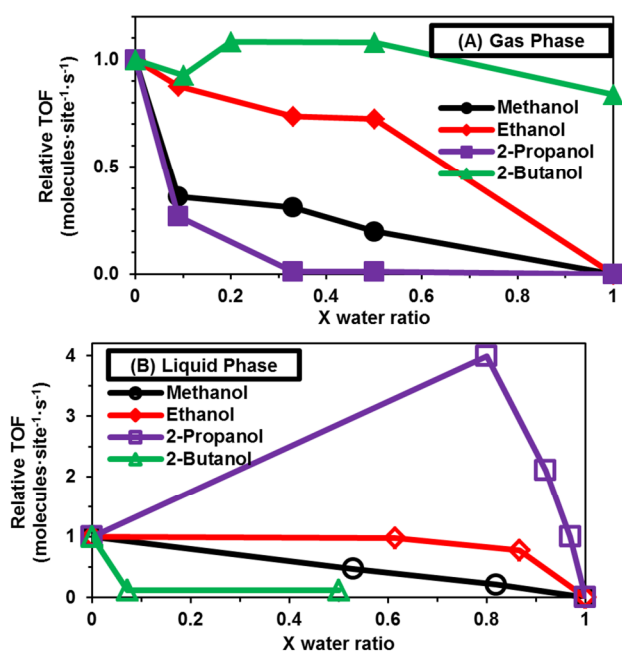

Figure 6. Water coadsorption effect on TOF of alcohol oxidation reactions (A) gas (10 Torr alcohol, 1-10 Torr water vapor, 50 Torr O_2, He as balance, in total 770 Torr, 60 °C, over 4 nm

(C1-C3 alcohol) and 6 nm (2-butanol) Pt/MCF-17) and (B) liquid phase (7.5-15 ml pure alcohol, 0-7.5 ml distilled water, in total 15 ml volume, C1-C3 alcohol: dissolved oxygen under 1 bar, 60 °C over 4 nm Pt/MCF-17, 2-BuOH: dissolved oxygen under 3 bar, 80 °C over 6 nm Pt/MCF-17)

The hydrophilicity of alcohol seems to be correlated with these phenomena. Methanol, ethanol and 2-propanol are miscible in water, while 2-butanol can be soluble by 12.5 g in 100 ml water due to the hydrophobic alkyl chain.[21] Pt NPs are covered by PVP capping agent which has amphiphilicity. In the gas phase where alcohol and water vapor can move freely, C1-C3 alcohol allows water to cover the Pt active site leading to poison the reaction progress. On the other hand, once 2-butanol attaches to the metal surface, it does not allow water to coadsorb on the catalyst. In the liquid phase where high concentrated alcohol exists around the catalyst, specific amount of water prompted the reaction turnover in 2-propanol oxidations. Meanwhile, water preferably gather around the catalyst due to the hydrophobicity of 2-butanol, poison the 2-butanol oxidations significantly in the liquid phase.
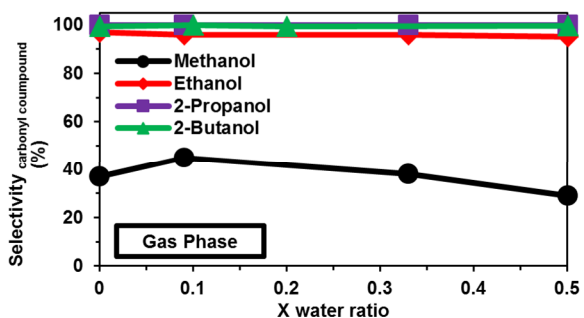

Figure 7. Water coadsorption effect on product selectivity of alcohol oxidation reactions in the gas phase (10 Torr alcohol, 1-10 Torr water vapor, 50 Torr O_2, He as balance, in total 770 Torr, 60 °C, over 4 nm (C1-C3 alcohol) and 6 nm (2-butanol) Pt/MCF-17)

Figure 7 shows the water coadsorption effect on the product selectivity in the gas phase. In the water-free methanol oxidation reaction, the selectivity was 37% of formaldehyde, and then went down gradually to 29% at the methanol to water ratio of 2:1. In C2-C4 alcohol oxidation reactions in the gas phase, the selectivity remained steady regardless of the water quantity. These results suggest that the water coadsoption does not affect the product selectivity under our conditions.

3.5. Sum frequency generation analysis

In order to clarify the reaction mechanism under different phase condition, we have examined SFG analysis about various alcohol species. Here 2-propanol oxidation SFG results was shown as below.

Figure 8 shows the correlation between reaction phase and 2-propanol molecular orientation on the catalyst surface. In the gas phase reaction condition, three vibrational peaks at ~2875 cm^{-1} (symmetric CH$_3$ stretch), ~2940 cm^{-1} (Fermi resonance), and ~2970 cm^{-1} (asymmetric CH$_3$ stretch) were detected. While in the liquid phase, the asymmetric stretch peak was increased and the symmetric stretch peak was decreased, which indicates the 2-propanol molecular orientation dependency on the reaction phase.
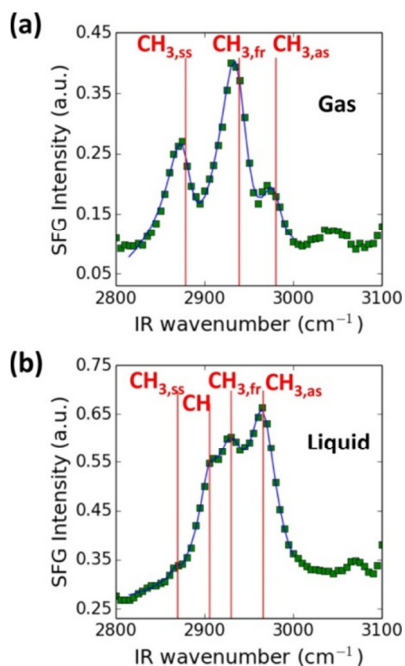
Figure 8. SFG spectra of gas (a) and liquid phase (b) 2-propanol on 4 nm Pt NPs under reaction conditions with O_2 and 60°C

3.6. DFT calculation

In order to reveal the alcohol molecular orientation possibility and how it affects to the reaction mechanism, DFT calculation was studied on 2-propanol oxidation reaction. Figure 9 shows that the minimum energy configurations of 2-propanol molecules on Pt (111) surface for the gas phase (a) and liquid phase (b) conditions. In the gas phase, the 2-propanol molecules preferably orient as "lying down" on the surface while "standing up" in the liquid phase. This conformation difference can be explained by molecular steric effect; molecules have to stand up for packing in high density liquid phase. Furthermore this phenomenon induces the different distance between β-hydrogen (β-H) of the 2-propanol and Pt surface. In the previous study on alcohol oxidation reaction, the rate-limiting step is believed to be the dissociation of methylene C-H in the alkoxide assisted by oxygen.[22,23] In the table 1, the β-H-Pt distance was 4.451Å for

14

the low concentrated condition, while 2.572Å for the high concentrated condition. It appears to be easier for the β-hydrogen to dissociate from the alkoxide species in the higher alcohol concentrated condition, which decreases the reaction activation energy in the liquid phase compared with that in the gas phase.
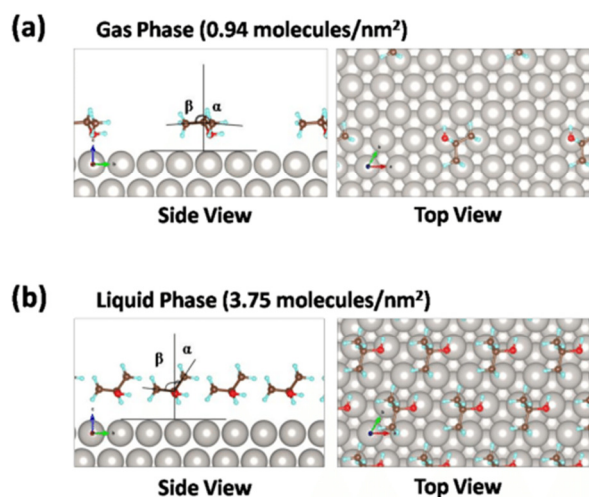

(a) Gas Phase (0.94 molecules/nm²)

Side View   Top View

(b) Liquid Phase (3.75 molecules/nm²)

Side View   Top View

Figure 9. DFT calculation for the minimum energy configurations of 2-propanol molecules on Pt (111) surface for the gas phase (a) and liquid phase (b) conditions (Pt-gray, C-brown, O-red, H-blue)

Table 1. 2-propanol molecular orientations as angles of C-C bonds relative to surface normal, adsorption energy, nearest surface-molecule distances, and nearest β-H-Pt distances for different concentrations of 2-propanol molecules on Pt (111) surface

Concentration (molecules/nm²)	α	β	E_{ads} (eV)	$R_{surf-mol}$ (Å)	H_{β}-Pt (Å)
0.94	86°	86°	-0.26	3.329	4.451
3.75	38°	84°	-0.12	3.905	2.572

4.   CONCLUSIONS

A wide variety of alcohol oxidation reactions with molecular oxygen over size-controlled Pt catalyst were discussed among methanol, ethanol, 2-propanol and 2-butanol. Generally, the turnover frequency increased with the catalyst particle size. The activation energies were similar with changes of the particle size and alcohol species but higher in the gas phases rather than those in the liquid phases. Water poisoned the catalyst surface and inhibited the oxidation reaction progress in the gas phases, while promoted the reaction in the liquid phases. The SFG and DFT analysis revealed that the alcohol molecule tends to pack horizontally on the metal surface in low concentration conditions, while it preferably stands up in high concentration conditions. The different molecular orientation of alcohol on the reaction active site affects the dissociation of the β-hydrogen of the alcohol and reaction activation energy. Further study on another alcohol oxidations catalyzed by Pt/MCF-17 is in progress and will be published soon.

ASSOCIATED CONTENT

Supporting Information

Detailed experimental procedures of Pt NPs synthesis, NPs size distribution and Pt/MCF-17 images are included. This material is available free of charge via the Internet at http://pubs.acs.org.

AUTHOR INFORMATION

Corresponding Author

*Phone: 510-642-4053. Fax: 510-643-9668

*E-mail: somorjai@berkeley.edu

Present Addresses

§BASF Corporation, 25 Middlesex/Essex Turnpike, Iselin, NJ 08830

⊥University of Szeged, Department of Applied and Environment Chemistry, Rerrich Bela ter 1,

H-6720 Szeged, Hungary

Author Contributions

‖These authors contributed equally.

Notes

ACKNOWLEDGMENT

REFERENCES

(1)   Sharma, A. S.; Kaur, H.; Shah, D.; Hutchings, G. J.; Haruta, M.; Haruta, M.; Haruta, M.; Haruta, M.; Hurata, M.; Kobayashi, T.; et al. Selective Oxidation of Alcohols by Supported Gold Nanoparticles: Recent Advances. *RSC Adv.* **2016**, *6* (34), 28688–28727.

(2)   Ciriminna, R.; Pandarus, V.; Béland, F.; Xu, Y.-J.; Pagliaro, M. Heterogeneously Catalyzed Alcohol Oxidation for the Fine Chemical Industry. *Org. Process Res. Dev.* **2015**, *19* (11), 1554–1558.

(3)   Kopylovich, M. N.; Ribeiro, A. P. C.; Alegria, E. C. B. A.; Martins, N. M. R.; Martins, L. M. D. R. S.; Pombeiro, A. J. L. Chapter Three – Catalytic Oxidation of Alcohols: Recent

Advances. In *Advances in Organometallic Chemistry*; 2015; Vol. 63, pp 91–174.

(4)   Feng, J.; Ma, C.; Miedziak, P. J.; Edwards, J. K.; Brett, G. L.; Li, D.; Du, Y.; Morgan, D. J.; Hutchings, G. J.; Davis, S. E.; et al. Au–Pd Nanoalloys Supported on Mg–Al Mixed Metal Oxides as a Multifunctional Catalyst for Solvent-Free Oxidation of Benzyl Alcohol. *Dalt. Trans.* **2013**, *42* (40), 14498.

(5)   Davis, S. E.; Ide, M. S.; Davis, R. J.; Donaldson, T. L.; Culberson, O. L.; Chheda, J. N.; Huber, G. W.; Dumesic, J. A.; Bozell, J. J.; Petersen, G. R.; et al. Selective Oxidation of Alcohols and Aldehydes over Supported Metal Nanoparticles. *Green Chem.* **2013**, *15* (1), 17–45.

(6)   Vinod, C. P.; Wilson, K.; Lee, A. F. Recent Advances in the Heterogeneously Catalysed Aerobic Selective Oxidation of Alcohols. *J. Chem. Technol. Biotechnol.* **2011**, *86* (2), 161–171.

(7)   Enache, D. I.; Edwards, J. K.; Landon, P.; Solsona-Espriu, B.; Carley, A. F.; Herzing, A. A.; Watanabe, M.; Kiely, C. J.; Knight, D. W.; Hutchings, G. J. Solvent-Free Oxidation of Primary Alcohols to Aldehydes Using Au-Pd/TiO2 Catalysts. *Science* **2006**, *311* (5759), 362–365.

(8)   Mallat, T.; Baiker, A. Oxidation of Alcohols with Molecular Oxygen on Solid Catalysts. *Chem. Rev.* **2004**, *104* (6), 3037–3058.

(9)   Ferri, D.; Baiker, A. Advances in Infrared Spectroscopy of Catalytic Solid–Liquid Interfaces: The Case of Selective Alcohol Oxidation. *Top. Catal.* **2009**, *52* (10), 1323–1333.

(10)   Wang, H.; An, K.; Sapi, A.; Liu, F.; Somorjai, G. A. Effects of Nanoparticle Size and Metal/Support Interactions in Pt-Catalyzed Methanol Oxidation Reactions in Gas and

Liquid Phases. *Catal. Letters* **2014**, *144* (11), 1930–1938.

(11) Sapi, A.; Liu, F.; Cai, X.; Thompson, C. M.; Wang, H.; An, K.; Krier, J. M.; Somorjai, G. A. Comparing the Catalytic Oxidation of Ethanol at the Solid–Gas and Solid–Liquid Interfaces over Size-Controlled Pt Nanoparticles: Striking Differences in Kinetics and Mechanism. *Nano Lett.* **2014**, *14* (11), 6727–6730.

(12) Wang, H.; Sapi, A.; Thompson, C. M.; Liu, F.; Zherebetskyy, D.; Krier, J. M.; Carl, L. M.; Cai, X.; Wang, L.-W.; Somorjai, G. A. Dramatically Different Kinetics and Mechanism at Solid/liquid and Solid/gas Interfaces for Catalytic Isopropanol Oxidation over Size-Controlled Platinum Nanoparticles. *J. Am. Chem. Soc.* **2014**, *136* (29), 10515–10520.

(13) Thompson, C. M.; Carl, L. M.; Somorjai, G. A. Sum Frequency Generation Study of the Interfacial Layer in Liquid-Phase Heterogeneously Catalyzed Oxidation of 2-Propanol on Platinum: Effect of the Concentrations of Water and 2-Propanol at the Interface. *J. Phys. Chem. C* **2013**, *117* (49), 26077–26083.

(14) Wang, H.; Wang, Y.; Zhu, Z.; Sapi, A.; An, K.; Kennedy, G.; Michalak, W. D.; Somorjai, G. A. Influence of Size-Induced Oxidation State of Platinum Nanoparticles on Selectivity and Activity in Catalytic Methanol Oxidation in the Gas Phase. *Nano Lett.* **2013**, *13* (6), 2976–2979.

(15) Tsung, C.-K.; Kuhn, J. N.; Huang, W.; Aliaga, C.; Hung, L.-I.; Somorjai, G. A.; Yang, P. Sub-10 Nm Platinum Nanocrystals with Size and Shape Control: Catalytic Study for Ethylene and Pyrrole Hydrogenation. *J. Am. Chem. Soc.* **2009**, *131* (16), 5816–5822.

(16) Schmidt-Winkel, P.; Lukens, W. W.; Yang, P.; Margolese, D. I.; Lettow, J. S.; Ying, J. Y.; Stucky, G. D. Microemulsion Templating of Siliceous Mesostructured Cellular Foams

with Well-Defined Ultralarge Mesopores. *Chem. Mater.* **2000**, *12* (3), 686–696.

(17)   Song, H.; Kim, F.; Connor, S.; Somorjai, G. A.; Yang, P. Pt Nanocrystals: Shape Control and Langmuir-Blodgett Monolayer Formation. *J. Phys. Chem. B* **2005**, *109* (1), 188–193.

(18)   Zhang, Y.; Grass, M. E.; Habas, S. E.; Tao, F.; Zhang, T.; Yang, P.; Somorjai, G. A. One-Step Polyol Synthesis and Langmuir-Blodgett Monolayer Formation of Size-Tunable Monodisperse Rhodium Nanocrystals with Catalytically Active (111) Surface Structures. *J. Phys. Chem. C* **2007**, *111* (33), 12243–12253.

(19)   Kaichev, V. V.; Popova, G. Y.; Chesalov, Y. A.; Saraev, A. A.; Zemlyanov, D. Y.; Beloshapkin, S. A.; Knop-Gericke, A.; Schlögl, R.; Andrushkevich, T. V.; Bukhtiyarov, V. I. Selective Oxidation of Methanol to Form Dimethoxymethane and Methyl Formate over a Monolayer V2O5/TiO2 Catalyst. *J. Catal.* **2014**, *311*, 59–70.

(20)   McCabe, R. W.; McCready, D. F. Kinetics and Reaction Pathways of Methanol Oxidation on Platinum. *J. Phys. Chem.* **1986**, *90*, 1428.

(21)   Alger, D. B. The Water Solubility of 2-Butanol: A Widespread Error. *J. Chem. Educ.* **1991**, *68* (11), 939.

(22)   Kobayashi, H.; Higashimoto, S. DFT Study on the Reaction Mechanisms behind the Catalytic Oxidation of Benzyl Alcohol into Benzaldehyde by O2 over Anatase TiO2 Surfaces with Hydroxyl Groups: Role of Visible-Light Irradiation. *Appl. Catal. B Environ.* **2015**, *170*, 135–143.

(23)   DiCosimo, R.; Whitesides, G. M. Oxidation of 2-Propanol to Acetone by Dioxygen on a Platinized Electrode under Open-Circuit Conditions. *J. Phys. Chem.* **1989**, *93* (2), 768–775.